

# Approximate two-body generating Hamiltonian for the PH-Pfaffian wavefunction

Kiryl Pakrouski<sup>1,2</sup>

<sup>1</sup>*Institute for Theoretical Physics, ETH Zurich, 8093 Zurich, Switzerland and*

<sup>2</sup>*Department of Physics, Princeton University, Princeton, NJ 08544*

(Dated: May 18, 2022)

We present two 2-body Hamiltonians that approximate the exact PH-Pfaffian wavefunction with their ground states for all the system sizes where this wavefunction has been numerically constructed to date. The approximate wavefunctions have high overlap with the original and reproduce well the low-lying entanglement spectrum and structure factor. The approximate generating Hamiltonians are obtained by an optimisation procedure where three to four pseudopotentials are varied in the neighbourhood of second Landau level Coulomb interaction or of a non-interacting model. They belong to a finite region in the variational space of Hamiltonians where each point approximately generates the PH-Pfaffian. We diagonalize the identified Hamiltonians for up to 20 electrons and find that for them the PH-Pfaffian shift appears energetically more favorable. Possibility to interpret the data in terms of composite fermions is discussed.

Fractional quantum Hall effect at the filling factor  $\nu = 5/2$  [1] is an interesting topological [2] state of matter that may potentially be used as a building block of a topological quantum computer [3, 4]. To large extent our understanding of the phenomenon rests on the model wavefunctions proposed to describe the state and their properties tested in experiment or numerically in small systems. Until recently the two leading candidate wavefunctions were the Moore-Read Pfaffian [5] and its particle-hole conjugate: anti-Pfaffian [6, 7]. The finite magnetic field used in experiment means finite energy difference between Landau levels [8] and leads to "Landau level mixing" that generates the particle-hole (PH) symmetry breaking terms in the effective models that could favour one of the two descriptions.

Although the two wavefunctions are topologically distinct, in the small systems the exact numerics is limited to, the competition between them is quite close. For example, including the first five PH-symmetry breaking terms one finds that Pfaffian is favoured [9] (see also [10, 11]) while a more precise model including first 6 [12] terms determines anti-Pfaffian (see also [13, 14]).

Particle-Hole symmetric Pfaffian (PH Pfaffian) [15] (also see a related earlier work [16]) is the third very recent candidate that has received support from some experimental observations [17, 18] but not from numerics [19–21] (in contrast to Pfaffian and anti-Pfaffian: [22–27]). Under the assumption that the signatures of the PH-Pfaffian never show up in the numerics and it thus can not be stabilised by any Hamiltonian relevant for  $\nu = 5/2$  a number of alternative scenarios explaining the quantized thermal Hall conductance  $\kappa_{xy}$  measurements [17] have been explored recently [28–41].

In this work, we report on a 2-body Hamiltonian that is a deformation of the second Landau level (SLL) Coulomb interaction and whose ground state approximates well the PH-Pfaffian wavefunction as written down in Ref. [28] in spherical geometry and in all the finite-size systems where this model wavefunction has been numerically constructed until now [42]. No such Hamiltonian has been reported to date [43] and we hope that it will be instrumental for further studies.

An optimisation approach [44] is used to determine the ap-

proximate 2-body generating Hamiltonian. It varies the pseudopotentials and searches the vicinity of a reference interaction for the points that are best according to a certain criteria or target function that is a weighted sum of the relevant properties. The highest contributions are given to the high overlap with the PH-Pfaffian wavefunction and small energy variance of the reference state  $(\sigma_E^{rel})^2 = \frac{\langle \psi_r | H_O^2 | \psi_r \rangle - \langle \psi_r | H_O | \psi_r \rangle^2}{\langle \psi_r | H_O | \psi_r \rangle^2}$ , which quantifies how close it is to being an eigenstate of the variational Hamiltonian. Further properties accounted in the search are: the total angular momentum of the ground state, gap, deviation from the reference interaction and ground state energy. All the system sizes where the model wavefunction is available (plus  $N_e=16$ ) are used and contribute to the target function being optimised proportionally to the size of their Hilbert space. As we work on the sphere at fixed  $L_z = 0$  we need to remember that the subspace, relevant for describing FQHE ground state, is given by the condition  $L = 0$ . There are 3;7;24;127  $L = 0$  states for systems with 6;8;10;12 electrons respectively. This ensures that the problem of "fitting" four variational parameters (pseudopotentials) is not trivial or over-parametrised as long as systems with at least 12 electrons are used (we use up to 16 electrons).

The Hamiltonian is parametrized by the 2-body pseudopotentials in spherical geometry [45]. The search is performed following the non-linear conjugate gradient descent algorithm with the Hestenes update rule (see [44] for details).

The method [44] can be viewed as mapping the variational parameters (pseudopotentials) into the feature space (Hilbert space) through diagonalizing the corresponding Hamiltonian and taking its ground state wavefunction. The overlap then defines a kernel in the feature space and other kernel methods of machine learning could potentially be used on top. Thus the method [44] may be considered a very simple example of the kernel-based Machine Learning [46].

We also have attempted to find the exact 2-body generating Hamiltonian following the "covariance matrix" methods [47–49] without success as zero eigenvalues required by these methods were absent for the covariance matrices constructed for the problem in question. This may be an indication that such an exact 2-body Hamiltonian doesn't exist and an ap-

TABLE I. The lowest pseudopotentials of the approximate PH Pfaffian generating Hamiltonians and the reference SLL Coulomb values. All higher pseudopotentials of CV7 are identical to the SLL Coulomb (values are given in Table S1) and are 0 for MV3.

	CV7	MV3	SLL Coulomb
$V_1$	1	1	1
$V_3$	0.694456627311176	0.433617799341989	0.773278825612202
$V_5$	0.665960300533016	0.370884676389928	0.576859542105588
$V_7$	0.448785272954577	0	0.487302680505104
$V_9$	0.52955224410569	0.164743667925535	0.433005097996708

proximate Hamiltonian such as the one presented in this work and found using [44] is the best one can do if restricted to 2-body terms only.

The approximate 2-body generating Hamiltonian is determined in the vicinity of the two reference interactions: SLL Coulomb given by the pseudopotentials computed for 20 electrons and the non-interacting system  $H = 0$ . In case of Coulomb we vary four pseudopotentials  $V_3$  through  $V_9$  while “freezing” all others to their reference values. In case of the “minimal model” we only vary three pseudopotentials  $V_3$ ,  $V_5$ ,  $V_9$ , while freezing the rest. Although one could achieve better fits varying more pseudopotentials it is commonly believed that usually only the lowest  $V_m$  with  $m \leq 9$  have physical significance. Another reason for limiting the number of variational parameters is the simplicity of the resulting model.

The optimisation results depend on the significance weights that we assign to various criteria contributing to the target function. Furthermore, because the optimisation problem is non-convex different results might in general be obtained for different initial conditions. Combined together this leads to a certain freedom as to what results should be identified as the best. In Table I we give two of the possible solutions with ids “CV7” (near SLL Coulomb) and “MV3” (minimal model).

Fig. 5 shows the learned pseudopotentials plotted together with the reference SLL and LLL Coulomb interactions. Compared to the SLL Coulomb  $V_5$  and  $V_9$  are the pseudopotentials that differ the most and this deformation is in the direction opposite to the LLL Coulomb (the named pseudopotentials are increased but would need to be decreased to obtain the LLL Coulomb). We also notice that in all the solutions we have obtained  $V_3$  and  $V_7$  are decreased and  $V_5$  and  $V_9$  are increased relative to the SLL Coulomb.

Table II contains the information on how close the Hamiltonians found are to being exact generating Hamiltonians of the PH-Pfaffian wavefunction. It lists the overlaps between the Hamiltonian ground state and the exact model wavefunction as well as the relative energy variance in exact PH-Pfaffian for individual system sizes. We also include the information on the LLL Coulomb that was noticed [19, 20] to provide a relatively large overlap with PH Pfaffian for 6 and 12 electrons. Relative energy variance quantifies how far a Hamiltonian is

TABLE II. Overlaps and energy variances for the two approximate generating Hamiltonians and the lowest Landau level Coulomb interaction

	MV3	CV7	LLL Coulomb
$\langle \psi_o   \psi_r \rangle (6)$	0.99142087	0.99210070	0.98628980
$\langle \psi_o   \psi_r \rangle (8)$	0.98009459	0.96521979	0
$\langle \psi_o   \psi_r \rangle (10)$	0.97161429	0.96271627	0
$\langle \psi_o   \psi_r \rangle (12)$	0.95538874	0.98570050	0.92987018
$\langle \psi_o   \psi_r \rangle (14)$	0.95878369	0.97167128	0
$(\sigma_E^{rel})^2 (6)$	2.4646E-4	1.4254E-5	1.3853E-4
$(\sigma_E^{rel})^2 (8)$	4.0823E-4	5.2169E-5	4.6648E-5
$(\sigma_E^{rel})^2 (10)$	2.1047E-4	1.4792E-5	3.6334E-5
$(\sigma_E^{rel})^2 (12)$	9.3918E-5	4.5660E-6	3.5453E-5
$(\sigma_E^{rel})^2 (14)$	1.6555E-4	8.4828E-6	1.7261E-5

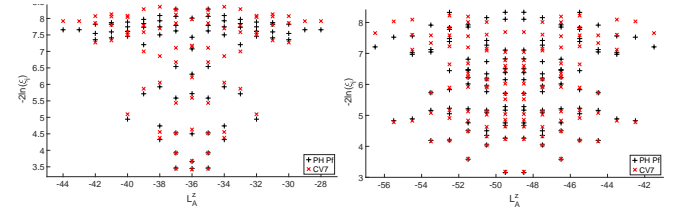


FIG. 1. Entanglement spectrum for 12 (Left Panel) and 14 (Right Panel) electrons computed in the model wavefunction and the ground state of the learned Hamiltonian near SLL Coulomb (CV7). The cut is made at the “equator” of the sphere.

from having a particular wavefunction as an eigenstate. To put these numbers in perspective we provide the same data for the second Landau level Coulomb interaction and the anti-Pfaffian model wavefunction in Table S5. We observe that the precision with which CV7 approximates PH-Pfaffian is not worse than the one for SLL Coulomb and anti-Pfaffian.

In Fig. 1 we show the entanglement spectra calculated for the ground state of CV7 and the exact PH-Pfaffian for 12 and 14 electrons. We observe that the structure of the low-lying levels is reproduced well. Analogous data for MV3 and the LLL Coulomb ground states is shown in Fig. S12 where one can observe that the learned Hamiltonians are substantially better than the LLL Coulomb in reproducing the structure of the PH-Pfaffian entanglement for 12 electrons (for 14 electrons the ground state of LLL Coulomb has  $L \neq 0$ ).

Fig. 2 shows the structure factor [50] as a function of  $Q = \sqrt{L^2/S}$  for 12 and 14 electrons computed in the model wavefunction and in the ground states of relevant Hamiltonians. We observe that the learned Hamiltonian CV7 is best at reproducing the original structure factor while the data obtained in the LLL Coulomb ground state shows more pronounced oscillations and also grows slower at small  $Q$  than all other data.

Although the two Hamiltonians CV7 and MV3 are visually quite different (Fig. 5) their ground states have relatively high

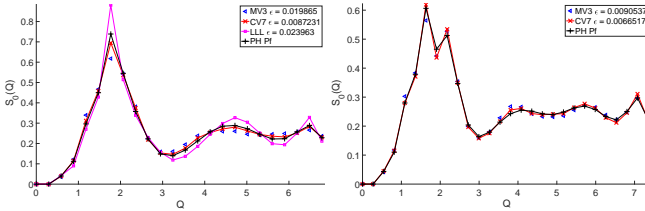


FIG. 2. Spectral form factor  $S_0(Q)$  for 12 (Left Panel) and 14 (Right Panel) electrons computed in the model PH-Pfaffian wavefunction and the ground states of the learned Hamiltonians and the LLL Coulomb interaction. The normalized deviation from the PH-Pfaffian data is  $\epsilon = \sum_{L=1}^{L_{max}} (|S_0(Q) - S_0^{PH Pf}(Q)|)/L_{max}$

overlap above 0.98 up to 20 electrons as can be seen in the Tab. S3.

If we interpolate between them  $H(\alpha) = (1 - \alpha)H_{MV3} + \alpha H_{CV7}$  (Fig. S2) we do not observe any sign of gap closing and the PH-Pfaffian overlap stays above 0.955 for all system sizes at all interpolation points. This suggests that the two Hamiltonians CV7 and MV3, actually belong to a single continuously connected region in the parameter space defining the Hamiltonians that approximately generate PH-Pfaffian [51]. This conclusion is supported by the entanglement spectrum data computed at every third interpolation step and shown in Fig. S3 for  $N_e = 12, 14$ . We observe that the original level counting of the PH-Pfaffian is preserved for every interpolation step. Similarly the low-lying entanglement spectra agree between CV7 and MV3 for  $N_e = 18, 20$  as shown in Fig. S1.

Blue crosses in Fig. 5 show the CV7 pseudopotentials shifted downwards by a constant equal to the largest pseudopotential that was used in the optimisation procedure  $V_{31}^{SLLCoul} = V_{31}^{CV7}$ . Note how close the resulting  $V_3$  and  $V_5$  become to the values in MV3. Together with  $V_9$  increased over  $V_7$  this might be the underlying general feature that is required for approximating PH-Pfaffian.

The available data indicates that the learned Hamiltonians CV7 and MV3 represent a reasonable approximation of the PH-Pfaffian wavefunction for the system sizes with up to 14 electrons. We will now attempt to extract additional information about the PH-Pfaffian state from these Hamiltonians. Note however, that this program may only be successful if the small system sizes we used for learning contained enough information representative of the PH-Pfaffian phase [44] which can not be verified before the PH-Pfaffian wavefunction for larger sizes is available.

*Physics of the approximate generating Hamiltonian.* First we would like to understand how the learned Hamiltonians compare to the Coulomb interaction in the first and second Landau levels.

When interpolating between SLL Coulomb and CV7 ( $H(\alpha) = (1 - \alpha)H_{Coul} + \alpha H_{CV7}$ ) we perform the diagonalisation at both the PH-Pfaffian and anti-Pfaffian shifts. For each of the system sizes we keep track of the neutral gap (difference between the lowest eigenvalues) and the overlap with

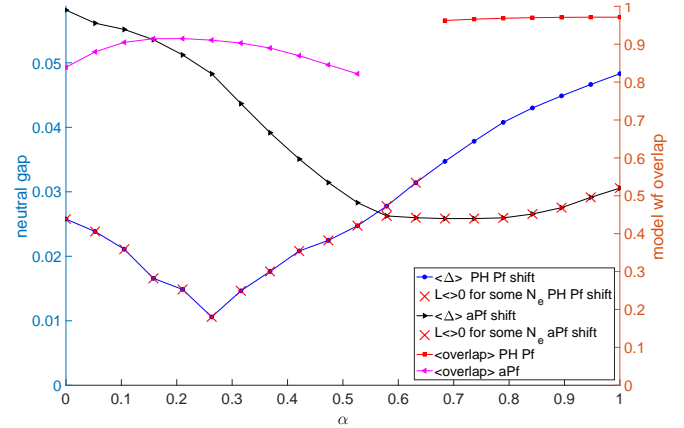


FIG. 3. Interpolation between the SLL Coulomb interaction ( $\alpha = 0$ ) and the learned Hamiltonian CV7 ( $\alpha = 1$ ). Overlap is averaged over systems with 8-14 particles and gap - over systems with 8-16 particles.

the relevant model wavefunction. Fig. 3 shows the cumulative averaged data for the system sizes with 8 to 16 electrons (holes). If at a given  $\alpha$  we find an  $L \neq 0$  ground state for any of the available system sizes (up to  $N_e=18$ ) we mark the gap with a red cross indicating that no fractional quantum Hall state is possible for that interaction at the corresponding shift.

Data for individual system sizes can be found in Fig. S7. While we observe some sort of phase transition accompanied by a gap closing for most system sizes this is not the case for the "closed shell" [42] systems such as 12 particles.

If the learned Hamiltonian CV7 is deformed in the direction of the LLL Coulomb the PH-Pfaffian state is destroyed much faster (see Fig. S8). For  $N_e = 18$  there is no single datapoint in that direction with  $L = 0$ , meaning no valid FQHE state is possible if we move towards LLL Coulomb. The system with 12 electrons again does not seem to close the gap during the interpolation while the first excited state changes from  $L = 6$  at LLL Coulomb to  $L = 2$  for CV7.

We conclude that the found Hamiltonian CV7 is a reasonable approximation for PH-Pfaffian in a finite region in the parameter space rather than at a single special point.

The neutral energy gaps for the two learned Hamiltonians are shown in the left panel of Fig. 4. The analysis is complicated by both the finite-size effects and the fact that the closed-shell systems with 6,12 and 20 electrons have much higher gaps as if they stemmed from a different dataset. Therefore the data doesn't seem to allow a reliable extrapolation and a conclusion if the corresponding states are gapped in the thermodynamic limit. For comparison we also show the more consistent data at anti-Pfaffian shift and SLL Coulomb interaction.

For CV7 we also compare the ground state energy at various shifts at fixed electron number (Fig. 4). We observe that the energy at the PH-Pfaffian shift is lower than the average of nearby flux values. For 12 electrons energy at the PH-Pfaffian shift is  $E(24) = 36.2963$  while the average of energies at

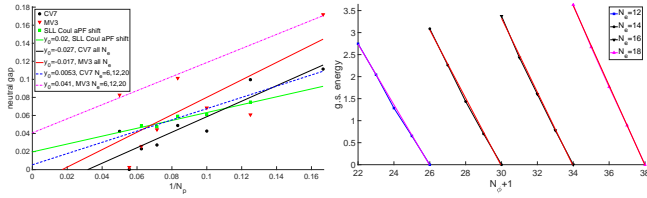


FIG. 4. Left Panel: Black circles and red triangles - energy gaps for the two learned Hamiltonians CV7 and MV3 and system sizes of 6 to 20 electrons. For each data set two linear fits are displayed: using all data points (black solid line for CV7 and red solid line for MV3) and using the "closed shell" sizes of 6,12,20 electrons (blue dashed line for CV7 and magenta dot-dashed line for MV3). Green squares - energy gaps for SLL Coulomb interaction at anti-Pfaffian shift computed for 8-16 holes. Right Panel: Lowest energy at the PH-Pfaffian and nearby shifts calculated for CV7 and  $N_e = 12, 14$ . For each  $N_e$  we subtract the energy at maximum flux to make them comparable. The linear fit shown in red and magenta is over the four points excluding the flux corresponding to the PH-Pfaffian shift.

the Pfaffian and anti-Pfaffian shifts is  $(E(22) + E(26))/2 = 36.3845$ . For 14 electrons corresponding energies are 47.5120 and 47.6207 again favouring PH-Pfaffian shift. The energies and angular momenta at various fluxes and electron numbers for CV7 and MV3 are listed in Table S4. The fact that  $L \neq 0$  at  $\pm 1$  flux is consistent with the PH-Pfaffian flux being most energetically favourable and the nearby states corresponding to quasiparticles.

The systems with  $N_e = 6, 12, 20$  electrons stand out by every possible measure. In Fig. 4 we observe that the neutral gap for these system sizes is significantly higher and extrapolates to a positive value while a linear fit including all data extrapolates to negative values. Note that the model wavefunctions themselves are also substantially different as can be seen from the structure factor plots in Fig. S6.

The special properties of these systems are consistent with them corresponding to closed-shell configurations of composite fermions [52] with the effective flux 1 where a system with  $(\tilde{n} + 1)(\tilde{n} + 2)$  electrons completely fills all  $\Lambda$ -levels up to  $\tilde{n}$  so that maximum filled level for  $N_e = 6, 12, 20$  is  $\tilde{n} = 1, 2, 3$ . Further numerical data consistent with this assumption is assembled in SM Sec. VI.

To discuss whether the state described by the model wavefunction and approximated by the ground states of the learned Hamiltonian is gapped we perform the scaling analysis of the structure factor  $S_0(Q)$  [50]. For a gapped state the structure factor should grow as  $Q^\alpha = L^\alpha S^{-\alpha/2}$  with  $\alpha \geq 4$  [53]. We take the two smallest values  $L^* = 2, 3$  and plot  $\ln(S_0(L^*))$  vs  $\ln(S)$ . For sufficiently large system sizes we should be able to read off  $-\alpha/2$  from the slope of the linear fit to the data. We do obtain  $\alpha \geq 4$  for such an analysis performed for the anti-Pfaffian model wavefunction and the large enough ( $N_h \geq 12$ ) systems (see the right panel of Fig. S5). However, as the linear fit using smaller system sizes shows (see Figs. S5 and S4) the answer wouldn't have been so clear even for the anti-Pfaffian had only the systems with  $N_h \leq 14$  been available.

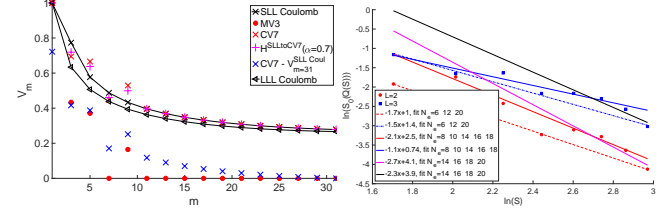


FIG. 5. Left Panel: Coulomb interaction in first and second Landau levels is shown with black triangles and crosses. Red circles and crosses are the learned Hamiltonians MV3 and CV7. Magenta "+" data indicates the interaction closest to SLL Coulomb that is still a reasonable approximation of PH-Pfaffian:  $0.3 * H^{SLLCoul} + 0.7 * H^{CV7}$ . Blue crosses correspond to the CV7 interaction shifted down by a constant  $-V_{31}^{SLLCoul}$ . Right Panel: Structure factor extrapolation over the ground states of the CV7 learned Hamiltonian.

As the previous literature suggested [19, 20, 42] the gap of the PH-Pfaffian must be much smaller should it be gapped. It is therefore to be expected that the "reliable" system size threshold is higher for the PH-Pfaffian.

Large finite-size effects in the CV7 data and the special behaviour of the closed-shell system sizes lead to several possible ways to linearly fit the available data some of which are shown [54] in Fig. 5 (data for MV3 is similar and is shown in the left panel of Fig. S5). The extracted  $\alpha$  and the qualitative result would depend on which data is used for the fit. Given this uncertainty we are not able to draw a solid conclusion and leave it (along with all the raw data available in SM) to the reader.

A related issue are the oscillations of the structure factor at large  $Q$  and the two-peak structure noted earlier [42] for the model PH-Pfaffian at some  $N_e$ . With the approximate wavefunctions we have access to larger system sizes and observe in Fig. S6 that the oscillations decrease and the two-peak structure becomes less pronounced for larger system sizes. It is thus possible that these two artefacts would be gone completely in larger systems. This assumption is substantiated by the comparison to the anti-Pfaffian data (bottom panel of Fig. S6) where the 8-hole structure factor resembles the double-peak structure and the 12-14-hole data exhibits remainder oscillations similar to the 20-electron PH-Pfaffian data.

*Conclusions and Outlook.* We presented two 2-body Hamiltonians that reasonably well approximate an implementation [42] of the PH-Pfaffian wavefunction on a sphere for all the system sizes where it is available. One of the Hamiltonians is a deformation of the second Landau level Coulomb interaction, the other - of a non-interacting model. Both Hamiltonians belong to a finite region of the four-dimensional Hamiltonian variational space where each point approximately generates PH-Pfaffian. Access to these microscopical models of PH-Pfaffian will enable multiple future studies of its relevance for the 5/2 fractional quantum Hall effect. Diagonalizing the Hamiltonians for up to 20 electrons we find that the finite-size effects improve; remain however present consistent with a gap much smaller than the one for anti-Pfaffian. The available data

neither supports nor excludes the possibility that the ground state of the approximate PH-Pfaffian-generating Hamiltonian is gapped. Larger system sizes are more consistent with a valid FQHE state by some measures. Access to several higher sizes of the model wavefunction and exact learned Hamiltonian eigenstates would be needed to gain certainty while we do not expect more than one additional system size to become accessible in the near future due to the computational complexity of the problem. Approximate methods might therefore be worth considering.

There are several interesting directions for the future investigation. Since there is no preferred way of constructing a PH-Pfaffian it would be reasonable to study other implementations than used in this work [28] and all prior literature. The presented Hamiltonian is a simplest 4-parameter model while adjusting further pseudopotentials would improve the approximation precision. An important open question is whether the required deformation of the Coulomb interaction may be obtained within some effective realistic model? For example, the pseudopotentials that perturbatively account for the Landau level mixing and finite width [10, 13, 55] to lowest order do not to our knowledge produce the suitable two-body corrections. It has been argued that 3-body pseudopotentials may be required to stabilize PH-Pfaffian [56–58] and it would be interesting to include 3-body and higher-order pseudopotentials into the variational Hamiltonian ansatz. The 2-body Hamiltonians presented here will be a valuable starting point for such a study.

It is also possible to modify the search/optimisation criteria that could lead to a PH-Pfaffian approximation with smaller overlaps but larger gaps or include new terms that would enforce the expected topological properties of PH-Pfaffian.

In case one is able to find a 3- plus 2-body Hamiltonian (breaking PH-symmetry) of which the PH-symmetric model wavefunction is an exact eigenstate it may also be possible to further deform this Hamiltonian [59, 60] such that the model wavefunction would not thermalize with the rest of the Hilbert space and become an example of a many-body scar state, the phenomenon also known as weak ergodicity breaking [61].

**Acknowledgements.** I gratefully acknowledge many useful discussions and the collaboration with E. Rezayi and F. D. M. Haldane during which the wavefunction used in this work was constructed. I also thank A. Balram for valuable discussions and comments on a version of this manuscript. This work was supported by DOE grant DE-SC0002140 and by the Swiss National Science Foundation through the Early Post-doc.Mobility grant P2E2P2\_172168. The simulations presented in this article were performed on computational resources managed and supported by Princeton’s Institute for Computational Science & Engineering and OIT Research Computing.

---

- [1] R. Willett, J. P. Eisenstein, H. L. Störmer, D. C. Tsui, A. C. Gossard, and J. H. English, Observation of an even-denominator quantum number in the fractional quantum hall effect, *Phys. Rev. Lett.* **59**, 1776 (1987).
- [2] X. G. Wen, Topological orders in rigid states, *International Journal of Modern Physics B* **04**, 239 (1990); X.-G. Wen, Theory of the edge states in fractional quantum hall effects, *International Journal of Modern Physics B* **06**, 1711 (1992).
- [3] C. Nayak, S. H. Simon, A. Stern, M. Freedman, and S. Das Sarma, Non-abelian anyons and topological quantum computation, *Rev. Mod. Phys.* **80**, 1083 (2008).
- [4] T. H. Hansson, M. Hermanns, S. H. Simon, and S. F. Viefers, Quantum hall physics: Hierarchies and conformal field theory techniques, *Rev. Mod. Phys.* **89**, 025005 (2017).
- [5] G. Moore and N. Read, Nonabelions in the fractional quantum hall effect, *Nuclear Physics B* **360**, 362 (1991).
- [6] M. Levin, B. I. Halperin, and B. Rosenow, Particle-hole symmetry and the pfaffian state, *Phys. Rev. Lett.* **99**, 236806 (2007).
- [7] S.-S. Lee, S. Ryu, C. Nayak, and M. P. A. Fisher, Particle-hole symmetry and the  $\nu = \frac{5}{2}$  quantum hall state, *Phys. Rev. Lett.* **99**, 236807 (2007).
- [8] That may be on the order of the intra-Landau-level Coulomb energy scale.
- [9] K. Pakrouski, M. R. Peterson, T. Jolicoeur, V. W. Scarola, C. Nayak, and M. Troyer, Phase diagram of the  $\nu = 5/2$  fractional quantum hall effect: Effects of landau-level mixing and nonzero width, *Phys. Rev. X* **5**, 021004 (2015).
- [10] M. R. Peterson and C. Nayak, More realistic hamiltonians for the fractional quantum hall regime in gaas and graphene, *Phys. Rev. B* **87**, 245129 (2013).
- [11] A. Wójs, C. Tóke, and J. K. Jain, Landau-level mixing and the emergence of pfaffian excitations for the 5/2 fractional quantum hall effect, *Phys. Rev. Lett.* **105**, 096802 (2010).
- [12] E. H. Rezayi, Landau level mixing and the ground state of the  $\nu = 5/2$  quantum hall effect, *Phys. Rev. Lett.* **119**, 026801 (2017).
- [13] S. H. Simon and E. H. Rezayi, Landau level mixing in the perturbative limit, *Phys. Rev. B* **87**, 155426 (2013); E. H. Rezayi and S. H. Simon, Breaking of particle-hole symmetry by landau level mixing in the  $\nu = 5/2$  quantized hall state, *Phys. Rev. Lett.* **106**, 116801 (2011).
- [14] M. P. Zaletel, R. S. K. Mong, F. Pollmann, and E. H. Rezayi, Infinite density matrix renormalization group for multicomponent quantum hall systems, *Phys. Rev. B* **91**, 045115 (2015).
- [15] D. T. Son, Is the composite fermion a dirac particle?, *Phys. Rev. X* **5**, 031027 (2015).
- [16] T. Jolicoeur, Non-abelian states with negative flux: A new series of quantum hall states, *Phys. Rev. Lett.* **99**, 036805 (2007).
- [17] M. Banerjee, M. Heiblum, V. Umansky, D. E. Feldman, Y. Oreg, and A. Stern, Observation of half-integer thermal hall conductance, *Nature* **559**, 205 (2018).
- [18] B. Dutta, W. Yang, R. A. Melcer, H. K. Kundu, M. Heiblum, V. Umansky, Y. Oreg, A. Stern, and D. Mross, Novel method distinguishing between competing topological orders (2021), *arXiv:2101.01419 [cond-mat.mes-hall]*.
- [19] R. V. Mishmash, D. F. Mross, J. Alicea, and O. I. Motrunich, Numerical exploration of trial wave functions for the particle-hole-symmetric pfaffian, *Phys. Rev. B* **98**, 081107 (2018).
- [20] A. C. Balram, M. Barkeshli, and M. S. Rudner, Parton construction of a wave function in the anti-pfaffian phase, *Phys. Rev. B* **98**, 035127 (2018).

[21] M. Yutushui and D. F. Mross, Large-scale simulations of particle-hole-symmetric pfaffian trial wave functions, *Phys. Rev. B* **102**, 195153 (2020).

[22] R. H. Morf, Transition from quantum hall to compressible states in the second landau level: New light on the  $\nu = 5/2$  enigma, *Phys. Rev. Lett.* **80**, 1505 (1998).

[23] E. H. Rezayi and F. D. M. Haldane, Incompressible paired hall state, stripe order, and the composite fermion liquid phase in half-filled landau levels, *Phys. Rev. Lett.* **84**, 4685 (2000).

[24] A. E. Feiguin, E. Rezayi, C. Nayak, and S. Das Sarma, Density matrix renormalization group study of incompressible fractional quantum hall states, *Phys. Rev. Lett.* **100**, 166803 (2008).

[25] M. R. Peterson, T. Jolicoeur, and S. Das Sarma, Finite-layer thickness stabilizes the pfaffian state for the 5/2 fractional quantum hall effect: Wave function overlap and topological degeneracy, *Phys. Rev. Lett.* **101**, 016807 (2008).

[26] X. Wan, Z.-X. Hu, E. H. Rezayi, and K. Yang, Fractional quantum hall effect at  $\nu = 5/2$ : Ground states, non-abelian quasi-holes, and edge modes in a microscopic model, *Phys. Rev. B* **77**, 165316 (2008).

[27] J. Zhao, D. N. Sheng, and F. D. M. Haldane, Fractional quantum hall states at  $\frac{1}{3}$  and  $\frac{5}{2}$  filling: Density-matrix renormalization group calculations, *Phys. Rev. B* **83**, 195135 (2011).

[28] P. T. Zucker and D. E. Feldman, Stabilization of the particle-hole pfaffian order by landau-level mixing and impurities that break particle-hole symmetry, *Phys. Rev. Lett.* **117**, 096802 (2016).

[29] S. H. Simon, Interpretation of thermal conductance of the  $\nu = 5/2$  edge, *Phys. Rev. B* **97**, 121406 (2018).

[30] C. Wang, A. Vishwanath, and B. I. Halperin, Topological order from disorder and the quantized hall thermal metal: Possible applications to the  $\nu = 5/2$  state, *Phys. Rev. B* **98**, 045112 (2018).

[31] D. F. Mross, Y. Oreg, A. Stern, G. Margalit, and M. Heiblum, Theory of disorder-induced half-integer thermal hall conductance, *Phys. Rev. Lett.* **121**, 026801 (2018).

[32] B. Lian and J. Wang, Theory of the disordered  $\nu = \frac{5}{2}$  quantum thermal hall state: Emergent symmetry and phase diagram, *Phys. Rev. B* **97**, 165124 (2018).

[33] S. H. Simon, M. Ippoliti, M. P. Zaletel, and E. H. Rezayi, Energetics of pfaffian–anti-pfaffian domains, *Phys. Rev. B* **101**, 041302 (2020).

[34] D. E. Feldman, Comment on “interpretation of thermal conductance of the  $\nu = 5/2$  edge”, *Phys. Rev. B* **98**, 167401 (2018).

[35] S. H. Simon, Reply to “comment on ‘interpretation of thermal conductance of the  $\nu = 5/2$  edge’”, *Phys. Rev. B* **98**, 167402 (2018).

[36] K. K. W. Ma and D. E. Feldman, Partial equilibration of integer and fractional edge channels in the thermal quantum hall effect, *Phys. Rev. B* **99**, 085309 (2019).

[37] J. Park, C. Spånslått, Y. Gefen, and A. D. Mirlin, Noise on the non-abelian  $\nu = 5/2$  fractional quantum hall edge, *Phys. Rev. Lett.* **125**, 157702 (2020).

[38] I. C. Fulga, Y. Oreg, A. D. Mirlin, A. Stern, and D. F. Mross, Temperature enhancement of thermal hall conductance quantization, *Phys. Rev. Lett.* **125**, 236802 (2020).

[39] S. H. Simon and B. Rosenow, Partial equilibration of the anti-pfaffian edge due to majorana disorder, *Phys. Rev. Lett.* **124**, 126801 (2020).

[40] H. Asasi and M. Mulligan, Partial equilibration of anti-pfaffian edge modes at  $\nu = 5/2$ , *Phys. Rev. B* **102**, 205104 (2020).

[41] K. K. W. Ma and D. E. Feldman, Thermal equilibration on the edges of topological liquids, *Phys. Rev. Lett.* **125**, 016801 (2020).

[42] E. H. Rezayi, K. Pakrouski, and F. D. M. Haldane, Energetics of the ph-pfaffian state and the 5/2-fractional quantum hall effect (2021), [arXiv:2103.12026 \[cond-mat.mes-hall\]](https://arxiv.org/abs/2103.12026).

[43] Although it has been argued [62] that in principle the PH-Pfaffian topological order can exist in a translationally and rotationally invariant system.

[44] K. Pakrouski, Automatic design of Hamiltonians, *Quantum* **4**, 315 (2020).

[45] F. D. M. Haldane, Fractional quantization of the hall effect: A hierarchy of incompressible quantum fluid states, *Phys. Rev. Lett.* **51**, 605 (1983).

[46] M. Schuld and N. Killoran, Quantum machine learning in feature hilbert spaces, *Phys. Rev. Lett.* **122**, 040504 (2019).

[47] E. Chertkov and B. K. Clark, Computational inverse method for constructing spaces of quantum models from wave functions, *Phys. Rev. X* **8**, 031029 (2018).

[48] M. Greiter, V. Schnells, and R. Thomale, Method to identify parent hamiltonians for trial states, *Phys. Rev. B* **98**, 081113 (2018).

[49] X.-L. Qi and D. Ranard, Determining a local Hamiltonian from a single eigenstate, *Quantum* **3**, 159 (2019).

[50] F. D. M. Haldane, The quantum Hall effect (Springer, New York, 1990) Chap. The Hierarchy of Fractional States and Numerical Studies, p. 303.

[51] Conditioned on the state at the two points MV3 and CV7 being gapped in the first place, as discussed later finite size effects prohibit a definitive answer.

[52] J. K. Jain, Composite-fermion approach for the fractional quantum Hall effect, *Phys. Rev. Lett.* **63**, 199 (1989).

[53] S. M. Girvin, A. H. MacDonald, and P. M. Platzman, Magneto-roton theory of collective excitations in the fractional quantum hall effect, *Phys. Rev. B* **33**, 2481 (1986).

[54] Fitting using all the system sizes (not shown) would give  $\alpha \approx 3.6$  for  $L = 2$  and  $\alpha \approx 2.6$  for  $L = 3$ .

[55] I. Sodemann and A. H. MacDonald, Landau level mixing and the fractional quantum hall effect, *Phys. Rev. B* **87**, 245425 (2013).

[56] L. Antonić, J. Vučicević, and M. V. Milovanović, Paired states at 5/2: Particle-hole pfaffian and particle-hole symmetry breaking, *Phys. Rev. B* **98**, 115107 (2018).

[57] S. Djurdjević and M. V. Milovanović, Model interactions for pfaffian paired states based on chern-simons field theory description, *Phys. Rev. B* **100**, 195303 (2019).

[58] M. V. Milovanović, S. Djurdjević, J. Vučicević, and L. Antonić, Pfaffian paired states for half-integer fractional quantum hall effect, *Modern Physics Letters B* **34**, 2030004 (2020), <https://doi.org/10.1142/S0217984920300045>.

[59] K. Pakrouski, P. N. Pallegar, F. K. Popov, and I. R. Klebanov, Many-body scars as a group invariant sector of hilbert space, *Phys. Rev. Lett.* **125**, 230602 (2020).

[60] K. Pakrouski, P. N. Pallegar, F. K. Popov, and I. R. Klebanov, Group theoretic approach to many-body scar states in fermionic lattice models (2021), [arXiv:2106.10300 \[cond-mat.str-el\]](https://arxiv.org/abs/2106.10300).

[61] M. Serbyn, D. A. Abanin, and Z. Papić, Quantum many-body scars and weak breaking of ergodicity, *Nature Physics* **10**.1038/s41567-021-01230-2 (2021).

[62] C. Sun, K. K. W. Ma, and D. E. Feldman, Particle-hole pfaffian order in a translationally and rotationally invariant system, *Phys. Rev. B* **102**, 121303 (2020).